AGU PUBLICATIONS

Water Resources Research

RESEARCH ARTICLE
10.1002/2014WR016600

Modeling chloride transport using travel time distributions at Plynlimon, Wales

Paolo Benettin[1], James W. Kirchner[2,3], Andrea Rinaldo[1,4], and Gianluca Botter[1]

[1]Dipartimento di Ingegneria Civile, Edile e Ambientale, Università degli studi di Padova, Padua, Italy, [2]Department of Environmental Systems Science, ETH Zürich, Zürich, Switzerland, [3]Swiss Federal Research Institute WSL, Birmensdorf, Switzerland, [4]Laboratory of Ecohydrology ECHO/IIE/ENAC, École Polytechinque Fédérale de Lausanne, Lausanne, Switzerland

Key Points:
- Accuracy in reproducing the hydrochemical response of the catchment
- Soil and ground water interplay drives water quality dynamics
- Erratic mean travel times are related to changing catchment features

Correspondence to:
P. Benettin,
paolo.benettin@dicea.unipd.it

Citation:
Benettin, P., J. W. Kirchner, A. Rinaldo, and G. Botter (2015), Modeling chloride transport using travel time distributions at Plynlimon, Wales, *Water Resour. Res.*, *51*, 3259–3276, doi:10.1002/2014WR016600.

Received 28 OCT 2014
Accepted 4 APR 2015
Accepted article online 8 APR 2015
Published online 8 MAY 2015
Corrected 22 JUN 2015

This article was corrected on 22 JUN 2015. See the end of the full text for details.

Abstract Here we present a theoretical interpretation of high-frequency, high-quality tracer time series from the Hafren catchment at Plynlimon in mid-Wales. We make use of the formulation of transport by travel time distributions to model chloride transport originating from atmospheric deposition and compute catchment-scale travel time distributions. The relevance of the approach lies in the explanatory power of the chosen tools, particularly to highlight hydrologic processes otherwise clouded by the integrated nature of the measured outflux signal. The analysis reveals the key role of residual storages that are poorly visible in the hydrological response, but are shown to strongly affect water quality dynamics. A significant accuracy in reproducing data is shown by our calibrated model. A detailed representation of catchment-scale travel time distributions has been derived, including the time evolution of the overall dispersion processes (which can be expressed in terms of time-varying storage sampling functions). Mean computed travel times span a broad range of values (from 80 to 800 days) depending on the catchment state. Results also suggest that, in the average, discharge waters are younger than storage water. The model proves able to capture high-frequency fluctuations in the measured chloride concentrations, which are broadly explained by the sharp transition between groundwaters and faster flows originating from topsoil layers.

1. Introduction

River hydrochemistry is largely regulated by transport processes that take place at whole-catchment scales. Watersheds are complex heterogeneous systems that receive atmospheric inputs from rainfall and also internally generate solutes through interactions between mobile and immobile phases [*Rinaldo and Marani*, 1987; *Anderson et al*., 2002; *Botter et al*., 2006; *Godsey et al*., 2009; *Thompson et al*., 2011; *Park et al*., 2013; *Kirchner and Neal*, 2013]. Solutes are then transported through soils and aquifers toward the channel network and the catchment outlet. While multidecadal hydrochemical data are essential to determine long-term export dynamics, high-frequency data sets prove particularly important for understanding event-scale dynamics which may cause rapid fluctuations in stream concentrations [*Kirchner and Neal*, 2013]. High-frequency measurements allow the identification of shifts in catchment behavior associated with variations in catchment connectivity caused by drying and wetting [*Tetzlaff et al*., 2014; *Smith et al*., 2013]. Similarly, stream hydrochemistry can be used to investigate the role of nonlinearities and thresholds in runoff generation [*Detty and McGuire*, 2010; *Gannon et al*., 2014]. This is especially true in headwater catchments, where geomorphic effects of river networks (like the in-stream mixing of water originating from spatially distinct source areas) [*Rinaldo et al*., 1991] can be disregarded and the critical role of hillslope processes is dominant.

The time-variant theory of travel time distributions [*Botter et al*., 2010; *Rinaldo et al*., 2011; *Botter et al*., 2011; *van der Velde et al*., 2012; *Benettin et al*., 2013a; *Harman*, 2015] is a relatively recent advance in the field of catchment hydrology that explicitly accounts for the temporal variability of flow, storage states, and mixing in catchments. This theory is in line with recent theoretical advances that conceptualize catchments as stochastic dynamical systems [*Kirchner*, 2009; *Botter et al*., 2009]. The main innovations consist in considering water parcels as a dynamic population that evolves within a defined hydrologic control volume, and in characterizing the outflows through their ability to sample individuals of different ages from the storage. The need for new tools that can capture the dynamic nature of catchments has led to many recent time-variant

approaches for estimating water age in real-world applications [*van der Velde et al*., 2010; *Birkel et al*., 2012; *McMillan et al*., 2012; *Hrachowitz et al*., 2013; *Davies et al*., 2013; *Benettin et al*., 2013b; *Harman and Kim*, 2014; *van der Velde et al*., 2015; *Birkel et al*., 2015]. One of the key results of these new approaches is that instantaneous travel time distributions are intrinsically nonsmooth curves. Their erratic character stems from the vagaries of nature in injection, retention, and leaching to streamflow, and could be captured by analytic descriptions that explicitly include in and out fluxes as forcings.

The availability of high-quality data sets, jointly with extensive information on soil features and biogeochemistry, make the Plynlimon watersheds an ideal place to test recent advances in water age theory. In particular, our main focus here is analyzing and modeling chloride concentrations at the catchment outlet during 1 year of high-frequency measurements, with a view toward clarifying physical processes. Chloride has been extensively used to investigate transport processes at the catchment scale [*Kirchner et al*., 2000; *Page et al*., 2007; *Shaw et al*., 2008; *Oda et al*., 2009; *Godsey et al*., 2010; *Kirchner et al*., 2010; *van der Velde et al*., 2010; *Hrachowitz et al*., 2013; *Benettin et al*., 2013b], because it can be often considered as a conservative tracer [see *Svensson et al*., 2012]. At Plynlimon, chloride mainly originates from sea salt in rainfall, cloud water, and aerosol dry deposition, resulting in mean streamflow concentrations of about 5−7 mg/L [*Neal and Kirchner*, 2000; *Kirchner and Neal*, 2013]. Such a concentration is significantly higher than background noise, but lower than the toxicity threshold for vegetation uptake [*Xu et al*., 1999], implying some active role of plant uptake in the underlying solute circulation [*Queloz et al*., 2015a, 2015b]. Still, the impact of vegetation on tracer transport is poorly understood [*Brooks et al*., 2010; *Penna et al*., 2013] and catchment-scale mixing processes cannot be quantified directly. Thus, hydrochemical models represent a useful tool to test hypotheses concerning physical processes that drive solute circulation in river basins.

The hydrochemical model developed in this paper, based on a travel time formulation of transport and calibrated against chloride concentration measurements, is used to: (i) estimate the water storage that contributes to discharge and solute mixing, (ii) understand the transport mechanisms that drive the temporal dynamics of stream chloride concentration, and (iii) estimate the age of water released by stream discharge under different wetness conditions. Our results demonstrate that coupling solute measurements and transport models can significantly improve our ability to quantify spatially distinct streamflow sources and catchment-scale mixing processes, and may eventually support the interpretation of emergent patterns in river hydrochemistry.

2. Data and Study Area

In this study, we analyze data from the Upper Hafren catchment, mid-Wales (UK), where the Centre for Ecology and Hydrology (CEH) conducted intensive measurement campaigns (2007–2009), aimed at taking high-frequency water quality measurements in precipitation and streamflow, spanning more than 40 elements of the periodic table [*Neal et al*., 2012, 2013; *Kirchner and Neal*, 2013]. The watershed is part of the Plynlimon catchments, which have been extensively studied for the last 40 years, resulting in a notable body of literature that documents their climatic and morphologic features and explores their hydrological and hydrochemical behavior [see *Kirby et al*., 1991, 1997; *Neal et al*., 2001; *Neal*, 2004; *Brandt et al*., 2004; *Marc and Robinson*, 2007, and references therein].

The Hafren catchment (3.7 km^2) is subdivided into an upper and lower part (Figure 1) corresponding to two distinct landscapes [*Neal et al*., 2010]. The Lower Hafren (LH) is a Sitka spruce forest plantation underlain by peaty podzol soils, whereas the Upper Hafren (UH) is a relatively undisturbed moorland catchment with some wetland areas. Both UH and LH catchment outlets were monitored during the measurement campaign. Our analysis focuses on the UH because its high-frequency water quality record is longer. Further information describing the UH can be found in *Neal et al*. [2010, 2011]. The contributing catchment is small (1.2 km^2) with elevations ranging from 533 m at the gauging station to 738 m at the upper divides. A peat soil of about 40 cm overlies highly fractured mudstone and shale bedrock. The bedrock is progressively less weathered with depth, but borehole investigations revealed volumetrically significant water at depths up to 35 m and hydrologically active fracture flow at depths up to 95 m [*Neal et al*., 1997; *Haria and Shand*, 2004; *Shand et al*., 2005].

The climate is generally wet, with annual average precipitation about 2650 mm. Although detailed evapotranspiration estimates are not available for UH, extrapolations from surrounding catchments [see *Marc and*

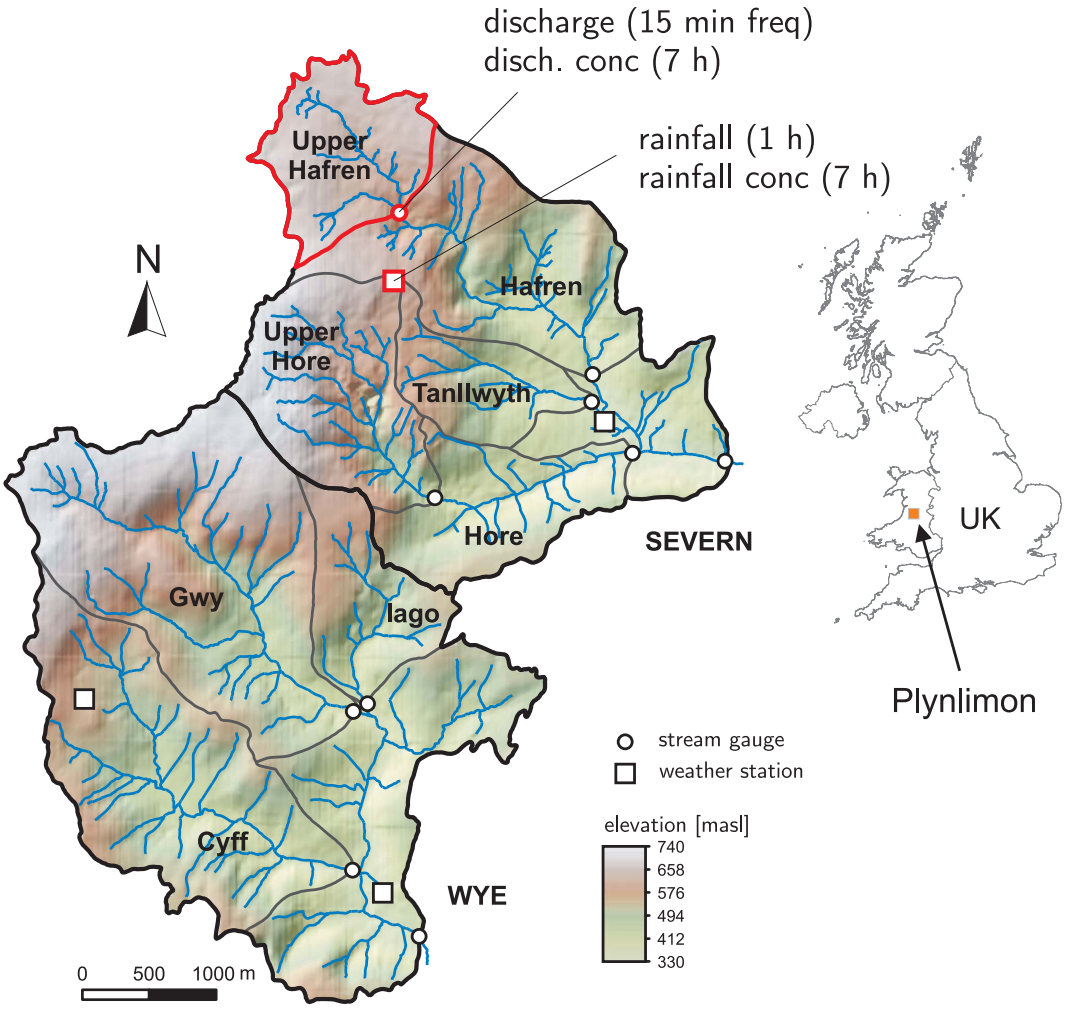

Figure 1. Map of the Plynlimon watersheds, obtained from a DTM.

Robinson, 2007] and a simple water balance based on precipitation and discharge measurements suggest that evapotranspiration may be 15% or less of precipitation. The hydrologic response is fast, with peak flows typically occurring within 1 h of precipitation and with a marked nonlinear relation between storage and discharge, as described by *Kirchner* [2009].

Chloride inputs are due to sea salt aerosols coming from the Atlantic Ocean, whose concentration can vary greatly from one storm to the next. The signal is markedly damped in discharge due to catchment transport processes that act as a fractal filter and convert white noise inputs into $1/f$ noise outputs [*Kirchner et al.*, 2000; *Kirchner and Neal*, 2013]. As shown by *Neal et al.* [2012], streamflow concentration displays time-varying correlations with discharge (Figure 2), with discharge peaks corresponding to both positive and negative fluctuations in chloride concentrations. This suggests the presence of a slowly varying base flow concentration that is temporarily increased/decreased by high-flow components characterized by a higher/lower concentration [*Neal et al.*, 2012]. The rationale behind this idea will be further explored with the aid of the model results (section 5).

To avoid some large gaps that occurred in the water quality measurements, our analysis spans the period from 22 December 2007 to 24 November 2008 (338 days) and comprises 1161 samples at 7 h intervals, including a few minor gaps. Over the same period, hourly rainfall measurements from the Carreg Wen station and 15 min discharges at the outlet are available. All water quality data are property of CEH and are freely available through their Information Gateway (https://gateway.ceh.ac.uk/).

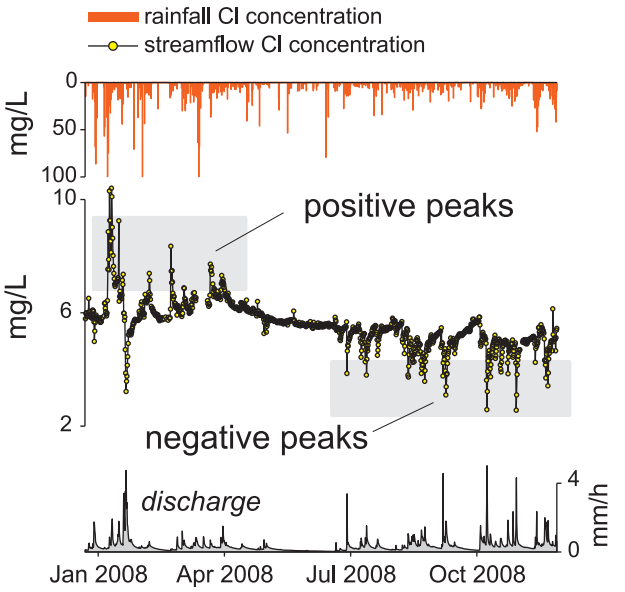

Figure 2. Chloride measurements over the considered period (22 December 2007 to 24 November 2008).

3. Overview of the Theoretical Approach

In this section, we briefly review the methods that are directly relevant to this study, while a full description of the theoretical basis upon which the model is built can be found in *Botter et al*. [2010, 2011] and *van der Velde et al*. [2012].

Let us consider a general system defined by a control volume V, crossed by input fluxes $IN(t)$ (typically rainfall) and output fluxes $OUT(t)$ (typically both evapotranspiration and discharge), that define the temporal dynamic of the storage $S(t)$ according to continuity. The age T of a water particle is the time elapsed since its entrance into the system, but we shall use two different terms to differentiate whether the age refers to a particle drawn from the storage or from the outflows. According to the terminology introduced by *McGuire and McDonnell* [2006], the age of a water particle in storage is termed residence time T_R to stress that the particle is still residing within the volume, hence its age can still grow. The exit age, instead, is called travel (or transit) time T_T, to stress that it pertains water particles that have completed their hydrologic journey within the control volume, as they are leaving the storage. Note that such notation and nomenclature, at times nearing a jargon, is not uniformly adopted in the literature, where the term residence time is sometimes used as a synonym of travel time. Two facts follow directly from the above definitions: (i) for any water particle, the travel time represents the maximum possible value of the residence time, as particles leaving the catchment cannot grow any older; (ii) when the input is sporadic (as rainfall forcings typically are), there cannot exist residence and travel times corresponding to periods with no input because no particles can exist with that age.

When considering many water particles traveling within the same control volume, the concept of residence and travel time leads to the definition of the residence time distribution (RTD) and travel (or transit) time distribution (TTD). TTDs can be interpreted in two different ways, depending on whether they track ages forward or backward in time [*Cvetkovic et al*., 2012]. In "forward" tracking, one selects a given particle injection at a fixed time t_i and follows the subsequent exit times. In "backward" tracking, instead, one focuses on a given exit time t_{ex}, considers the particles that leave the system at t_{ex} and then tracks their various entrance times backward in time. Although traditional transport approaches considered strictly forward distributions [e.g., *Danckwerts*, 1953; *Kreft and Zuber*, 1978], backward distributions are typically more suitable for studying streamflow measurements at an outlet, as they reflect inputs and transport processes that occurred prior to the sampling time. Forward and backward TTDs can be related by continuity [*Niemi*, 1977]. The RTD represents the distribution of the ages available within the storage at a given time t and, because it is based on the sequences of inputs that occurred prior to t, it is a backward distribution. In this study, we will only use backward distributions, denoting them with the following notation: $p_S(T,t)$ for the RTD and $p_Q(T,t)$ for the backward TTD. The notation stresses that these functions are time-dependent probability densities, defined over the age domain.

As the RTD represents the age storage of the catchment (normalized by the water storage amount), it serves as an age source for the outflows. Hence, assessing the set of ages preferentially removed from the storage (with respect to those available) is a meaningful way to characterize catchment-scale transport processes and can be performed by looking at how the TTD differs from the RTD. Such a difference can be studied

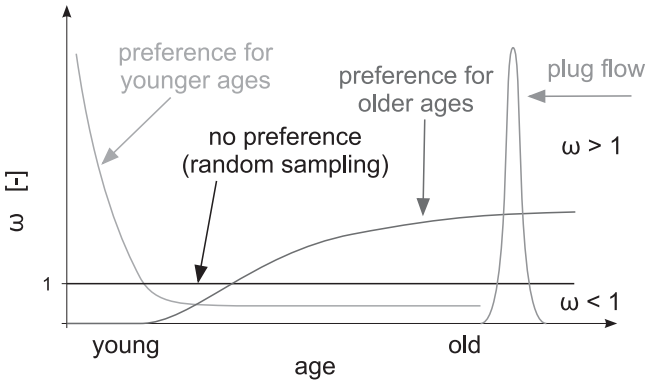

Figure 3. Example of possible shapes for the StorAge Selection functions $\omega(T,t)$.

through the ratio between the two distributions, resulting in the definition of the StorAge Selection (SAS) functions ω, introduced by *Botter et al.* [2011] (where they were originally referred to as "age-mixing" functions) and further investigated in *Botter* [2012], *van der Velde et al.* [2012], and *Harman* [2015]:

$$\omega(T,t)=\frac{p_Q(T,t)}{p_S(T,t)},\quad p_S(T,t)>0 \tag{1}$$

Examples of SAS functions are illustrated in Figure 3. For every age T, the benchmark value is $\omega=1$, indicating that such age is sampled by the outflows in the same proportion as it is contained within the storage. Otherwise, when $\omega>1$ ($\omega<1$), the considered age is oversampled (undersampled) by the outflows. Three main characteristic shapes can be thus identified in catchments (see Figure 3): (i) preference for younger ages, as a result of the mobilization of younger particles stored, e.g., in shallow soils, (ii) no preference (random sampling, $\omega=1$), occurring when dispersion is enhanced [*Benettin et al.*, 2013a] and discharge is a representative sample of the stored ages, (iii) preference toward older ages, when younger water is present but not mobilized, e.g., during late recessions.

SAS functions are spatially integrated descriptors of catchment processes and allow for the identification of general transport features, regardless of the specific input-output sequence considered in the study. Moreover, they can be used to define the dynamic linkage between the age distributions of storage and fluxes [*Botter et al.*, 2011], thereby shifting the focus from the TTDs to the underlying age-selection processes that generate such TTDs. This may be a promising avenue for the development of a general catchment theory.

Despite the intuitive essence of the formulation and the advances achieved by using a transformed travel time domain [*van der Velde et al.*, 2012; *Harman*, 2015], the use of SAS functions is still a challenge, because few real-world applications have been proposed in the literature and numerical solutions can be computationally demanding. A compelling alternative is to model the catchment through a series of physically meaningful storage partitions (typically, one for the shallow soil and one for deeper groundwaters) and assume a random sampling (RS) mixing scheme within each storage. This enables the use of analytical solutions that are particularly easy to implement. Moreover, the RS assumption was shown to give reasonable results in systems with high degrees of heterogeneity [*Benettin et al.*, 2013a; *Ali et al.*, 2014] and has been successfully applied to different settings [*Bertuzzo et al.*, 2013; *Benettin et al.*, 2013b] including comparisons to spatially distributed 3-D numerical models [*Rinaldo et al.*, 2011]. Under the RS approximation, the SAS function is equal to unity, hence the travel and residence time distributions coincide [*Botter*, 2012; *Hrachowitz et al.*, 2013] and can be expressed as:

$$p_Q(T,t)=p_S(T,t)=\frac{IN(t-T)}{S(t-T)}\exp\left(-\int_{t-T}^{t}\frac{OUT(\tau)}{S(\tau)}d\tau\right) \tag{2}$$

The related formulas for the computation of TTDs in multi-RS systems can be found in *Benettin et al.* [2013b, Appendix A].

The variability of TTDs over time is naturally induced by the time variability of hydrologic fluxes (see equation (2)). Nevertheless, it is equally interesting to provide time-invariant descriptors of transport at catchment scale that are able to summarize some "typical" behavior of the system. To this end, one can compute an ensemble average of individual TTDs over specific catchment states or during prescribed periods of interest, e.g., dry/wet periods [*Botter et al.*, 2010], seasons, or the entire period of record [*Heidbuechel et al.*, 2012]. This time averaging is a marginalization of the TTD over time (see Appendix A) and can help in characterizing the system behavior as a function of the underlying catchment state.

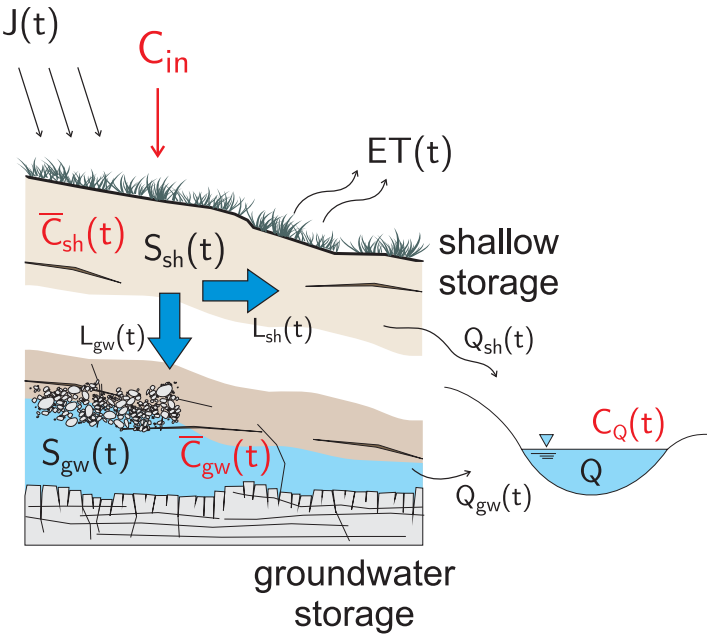

Figure 4. Conceptual catchment representation.

4. Hydrochemical Model of Upper Hafren and Its Parameter Calibration

A simple hydrochemical model was developed to simulate chloride transport at Upper Hafren. The model is similar to that used in *Benettin et al.* [2013b] and is made up of a hydrological and a transport component: the hydrological model is needed to estimate water fluxes and storages over the simulation period, while the transport model describes the evolution of chloride concentrations within the catchment and in the outflows.

4.1. Hydrologic Model

Previous studies of the Hafren catchment [e.g., *Shand et al.*, 2005; *Haria and Shand*, 2006] inspired us to conceptualize the catchment as a two-layer system, characterized by a shallow and a deep component (Figure 4).

The shallow layer includes both the upper portion of the fractured bedrock and the soil, which are relatively uncompacted and fast responding. The major hydrologic fluxes included in the model are precipitation (*J*), evapotranspiration (*ET*), and leakage (*L*) (that includes both lateral and vertical subsurface flows, as explained below). All precipitation is assumed to infiltrate into the soil except when the shallow layer is fully saturated. Leakage production is modeled through a non linear storage-discharge relationship [*Brutsaert and Nieber*, 1977] of the kind $L=aS_{sh}^{b_{sh}}$, where S_{sh} represents the dynamic water storage of the shallow layer, i.e., the volume of water that is mobilized during the hydrologic response, which can be computed through a hydrologic balance [*Birkel et al.*, 2011]. A fraction $\beta(t)$ of the leakage is assumed to flow laterally and discharge directly into the stream as shallow subsurface flow Q_{sh}, while the remaining fraction $(1-\beta(t))$ recharges the deep groundwater system. Overland flow seldom occurs in the model simulation, hence subsurface flow results as the dominant shallow component. To ensure that during wet periods, a higher fraction of the leakage drains directly into the stream, the partitioning term $\beta(t)$ is assumed to be storage dependent and it is computed as the product between a coefficient β_0 and the dynamic storage normalized by the root zone pore volume, $S_{sh}(t)/(nZ_r)$. Evapotranspiration has a minor role in the Upper Hafren catchment and was simply assumed equal to a reference value ET_{ref}, multiplied by a temperature-based correction factor that accounts for daily and seasonal variations in vapor pressure deficit and net radiation. The main model equations are summarized in Figure 5.

The deep layer is meant to represent the deep groundwater system and it includes the aquifer and the parent material underlying the highly fractured bedrock. The deep system is fed by vertical flow from the

	storage equation	inflows	discharge	evapotranspiration
shallow storage	$\frac{dS_{sh}}{dt} = J(t) - L(t) - ET(t)$	$J(t)$	$L(t) = a\left(\frac{S_{sh}(t)}{nZ_r}\right)^{b_{sh}}$	$ET(t) = ET_{ref}\frac{T(t)+30}{T(t)+30}$
groundwater storage	$\frac{dS_{gw}}{dt} = L_{gw}(t) - Q_{gw}(t)$	$L_{gw}(t) = [1-\beta(t)]\,L(t)$	$Q_{gw}(t) = a\left(\frac{S_{gw}(t)}{S_{max}}\right)^{b_{gw}}$	—

Figure 5. Hydrologic model equations.

shallow storage, while the only output is groundwater discharge, because evapotranspiration from the deep storage is neglected. In analogy with the shallow layer, groundwater flow from the deep system is modeled through a nonlinear storage-discharge relationship $Q_{gw}=aS_{gw}^{b_{gw}}$, where S_{gw} represents the dynamic groundwater storage. The use of four independent parameters to define the relevant storage-discharge relations (for the shallow storage and the groundwater) leads to equifinality because different combinations of a and b provide very similar Q-S curves in the range of discharges that pertain to each storage partition. Hence, to improve the identifiability of the parameters (and reduce their number), we assumed that the coefficient a in the two storage-discharge relations is the same, thereby removing 1 degree of freedom in the system characterization. The different behaviors of the two systems are then completely defined by the exponents b_{sh} and b_{gw}. This arbitrary choice has little impact on the overall model performance. Note that, even though for purely hydrologic purposes one nonlinear storage would provide satisfying results, the second storage is crucial to reproducing the observed chemical transport dynamics [see *Benettin et al.*, 2013b, section 7]. For ease of computation, the shallow and deep dynamic storages were made dimensionless. The former was scaled to the specific pore volume nZ_r, while the latter was scaled to a constant, S_{max}, explicitly designed to be larger than the maximum modeled S_{gw}. The normalization also allows the units of the a coefficient to be mm/h.

4.2. Chloride Circulation Model

The transport component of the model aims at describing chloride concentration dynamics in storages and outflows.

The measured rainfall concentration C_J was used as model input after some adjustments to account for the adopted sampling arrangement, as described in Appendix B. A second chloride input to the Plynlimon catchments is dry deposition, which is enhanced by the vegetation surface area [*Neal and Kirchner*, 2000]. However, we did not model dry deposition explicitly because, due to the large size of the sample collection funnel, sampled precipitation is likely to include its contribution.

As water infiltrates into the soil, it mixes with water already contained in the shallow storage. The size of this storage has a huge influence on solute circulation, because it defines the storage capacity of the shallow system (and thus its chemical memory). The total storage size cannot be computed from hydrologic models, which are sensitive only to the dynamic storage that is mobilized during the hydrologic response [*Kirchner*, 2009]. The remaining portion of storage, which is not hydrologically active, is usually referred to as residual storage or passive storage [*Birkel et al.*, 2011] and plays a critical role in the chemical response of watersheds because it can store solutes on time scales that are much longer than the time scale of hydrologic response. Hence, in both the shallow and the deep system, we model the actual storage $W(t)$ as the sum of a dynamic storage $S(t)$ and a residual storage W_0, which is assumed to be constant for simplicity. The residual storage is assessed through calibration based on observed chloride concentrations and has no influence on the hydrologic response. Hence, it can be effectively considered as a transport parameter.

The outflowing chloride concentration depends on how the outflows sample water parcels from the storage. This is simulated in the model by assigning the StorAge Selection function $\omega(T,t)$ to the relevant outflows from each compartment. The random sampling scheme employed in this study involves a selection function constantly equal to unity (see section 3), implying that every age is sampled from each storage compartment based on its relative abundance (the larger the volume of water in storage that shares a given age, the more that age is sampled). Under this assumption, and neglecting possible effects due to evapoconcentration (see later discussion on this issue), outflow concentrations can be expressed as [*Benettin et al.*, 2013b]:

$$C_{out}(t)=\int_0^\infty C_{in}(t-T)\,p_Q(T,t)dT=\int_0^\infty C_{in}(t-T)\,p_S(T,t)dT=\bar{C}(t) \tag{3}$$

where $\bar{C}(t)$ is the average storage concentration, which can also be computed as the ratio between mass and storage, $\bar{C}(t)=M(t)/(S(t)+W_0)$, with significant computational benefits. In the model, each outflow is assumed to randomly sample the corresponding storage. Hence, shallow subsurface flow and groundwater concentrations are obtained as the average concentration in the shallow system, $\bar{C}_{sh}(t)=M_{sh}(t)/(S_{sh}(t)+W_{0_{sh}})$, and in the groundwater, $\bar{C}_{gw}(t)=M_{gw}(t)/(S_{gw}(t)+W_{0_{gw}})$. Then, streamflow

concentrations $C_Q(t)$ are obtained by combining the shallow and groundwater components as a weighted average of $\bar{C}_{sh}(t)$ and $\bar{C}_{gw}(t)$:

$$C_Q(t) = \left(\frac{Q_{sh}(t)}{Q(t)}\right)\bar{C}_{sh}(t) + \left(\frac{Q_{gw}(t)}{Q(t)}\right)\bar{C}_{gw}(t) \tag{4}$$

Evapotranspiration was initially assumed to randomly sample water from the shallow layer with a concentration that is a fraction $\alpha \leq 1$ of the average storage concentration. This coefficient is designed to include the possible effects of selective evapotranspiration in case of potentially toxic solutes, which would lead to an increased storage concentration during warmer periods. However, when chloride concentrations in soil moisture are below toxic levels, chloride is taken up by plants for metabolic and biochemical functioning [see *Xu et al.*, 1999]. Preliminary calibrations suggested optimal values of α in the range $0.9-1$ (implying no evapoconcentration), in line with observational data that do not show any evidence of evapoconcentration during the warmest months of the simulation period (May to August 2008). Hence, to reduce the number of parameters, we decided not to model evapoconcentration and kept $\alpha = 1$ (thus implying that transpired water has the same chloride concentration as the average shallow storage), leaving the two residual storages $W_{0_{sh}}$ and $W_{0_{gw}}$ as the only transport parameters that require calibration.

It is important to note that even though the two storages are individually randomly sampled, the overall catchment is not, because water is distributed differently between the upper and lower reservoirs. For example, younger ages can be a small fraction of the overall storage as they are mainly confined in a smaller shallow reservoir, yet they can dominate the catchment discharge if stormflow is mainly made of soil water. This key issue is described in detail in section 6.

4.3. Model Calibration

The hydrochemical model described in the previous section was implemented by using a forward semianalytical approach. For each partition of the storage, the hydrologic balance is solved, at any time step, implementing the analytic solution of the mass balance equation based on the underlying storage-discharge relationship. In the shallow system, a small fraction of the storage is also removed by evapotranspiration. The mass balance is then computed by multiplying each hydrologic flux by the corresponding chloride concentration at the considered time step. In doing so, measured chloride in precipitation is uniformly downscaled from 7 to 1 h time step. All the outflows are assumed to be characterized by the mean storage concentration computed at the previous time step, which is a by-product of the RS assumption. The chloride mass stored within each compartment is updated according to the computed fluxes and then divided by the corresponding water storage (also including the residual component) to obtain the updated mean storage concentration. Chloride contained within the catchment storage at the beginning of the simulation is accounted for through the initial conditions $\bar{C}_{sh}(t=0)$ and $\bar{C}_{gw}(t=0)$. A warm-up period is employed at the beginning of the simulations to reduce the impact of the initial conditions on the model results.

The estimate of water and solute fluxes in the system requires the determination of the model parameters. Some of them were set a priori based on previous analyses and field surveys [e.g., *Neal et al.*, 2010] as summarized in Table 1. The remaining parameters were estimated through a Markov Chain Monte Carlo (MCMC) calibration procedure using *DREAM*$_{ZS}$ [*Vrugt et al.*, 2009; *ter Braak and Vrugt*, 2008]. The calibration parameters comprise five hydrologic parameters (three for the storage-discharge relationships, one for the leakage partitioning, and one for evapotranspiration) and two transport parameters (the two residual storages), as summarized in Table 2. The hydrological and transport parameters were calibrated separately, according to the procedure described in the following.

Hydrologic parameters were calibrated against hourly discharge data. The objective function that we implemented in the MCMC is the standard log-likelihood function:

$$logL = \frac{N}{2}\log(2\pi) - N\log(\sigma_e) - \sum_{i=1}^{N}\frac{\epsilon_i^2}{2\sigma_\epsilon^2} \tag{5}$$

where N is the number of measurements, ϵ_i is the model error at time i (calculated as the residual $Q(i) - Q_{obs}(i)$), and σ_e is the error standard deviation. The use of equation (5) is based on the assumption of independent and identically distributed Gaussian errors. Even though these assumptions (especially the

Table 1. Constant Parameters

Parameter	Symbol	value
Soil porosity	n	0.35
Root zone depth (mm)	Z_r	400
Max gw storage (mm H_2O)	S_{max}	1000
Initial gw conc. (mg/L)	$\bar{C}_{gw_0}$	5.4

lack of error correlation) are unlikely when dealing with discharge or concentration time series, more sophisticated objective functions would require more parameters to be estimated, without completely avoiding the problem of introducing arbitrary assumptions at some point. To account for the loss of degrees of freedom induced by serial error correlation, we used an increased error standard deviation $\sigma_e = 1$ mm/h. As 5 years of discharge measurements are available at the Upper Hafren, we could compare the parameters' posterior distributions resulting from the calibration of individual years. The obtained distributions generally overlap (Figure 6a), indicating mutual consistency of our estimates across different years. This served as an independent verification of the reliability of the calibrated parameters provided by the MCMC algorithm. Consistently, a single calibration for the entire data set of 5 years resulted in a narrower distribution, peaking where the individual distributions overlap. Moreover, the optimal set obtained during the 5 year calibration performs well in each individual year (see Table 3), so it was selected and kept constant for chemical calibration and for the travel time analysis.

Transport parameters were calibrated against chloride measurements using the likelihood function provided by equation (5) with $\sigma_e = 1.5$ mg/L. Again, the error standard deviation was adjusted to account for the observed serial correlation in the residuals. As just 1 year of high-frequency chloride measurements is available, it has been entirely used for calibration. In the absence of validation periods, calibrated residual storage parameters are less suitable for longer-term transport processes. The posterior distributions of the chemical parameters (Figure 6b) show that the residual component of the shallow storage is well identified ($W_{0sh} \approx 500-600$ mm H_2O) and consistent with field observations of the fractured bedrock depth [*Shand et al*., 2005]. In contrast, groundwater residual storage is much more uncertain ($W_{0gw} > 1500$ mm H_2O), owing to the strong filtering of high-frequency information in the input signal by groundwater storage. The uncertainty in the size of the groundwater storage may be aggravated by the brevity of the simulation in our modeling exercise (approximately 1 year). Nonetheless, the total residual storage implied by our model is consistent with the estimate by *Kirchner et al*. [2000] of a mean travel time of 0.9 years in the Hafren catchment, which equals approximately 2000 mm of storage (0.9 years times 2650 mm/yr of precipitation, minus 15% evapotranspiration). Implications of the uncertainty in the deep residual storage are discussed in sections 5 and 6.

5. Results

The calibrated hydrochemical model was run over the December 2007 to November 2008 period. Simulated discharge and its partition into shallow layer and groundwater contributions are shown along with observed flows in Figure 7. Nash-Sutcliffe (NS) efficiencies are 0.94 for discharge and 0.91 for log-discharge, indicating that the model is able to capture both the peaks and the recessions of the observed hydrograph. The flow partitioning shows that hydrograph peaks are dominated by drainage from the shallow layer, while the groundwater, though quite reactive during wet periods, accounts for most of the recessions. The simulated chloride concentration is shown in Figure 8. Besides the first negative peak in the observed time series, which might be due to the occurrence of overland flow or other processes that could not be properly simulated by this simple model, all dilutions taking place after June 2008 are well reproduced by the model.

Table 2. Calibration Parameters[a]

Parameter	Symbol	Low. Bound	Upp. Bound	Calib. Value
Reference ET (mm/h)	ET_c	0	0.15	0.025
Leakage partitioning	β_0	0	2.5	0.85
SD coeff. (mm/h)	a	10^{-1}	10^4	$10^{1.3}$
SD exponent sh	b_{sh}	0	30	7.9
SD exponent gw	b_{gw}	0	80	28.0
Residual storage sh (mmH_2O)	W_{sh}	100	1000	540
Residual storage gw (mm H_2O)	W_{gw}	100	5000	2700

[a]SD = storage-discharge relationship.

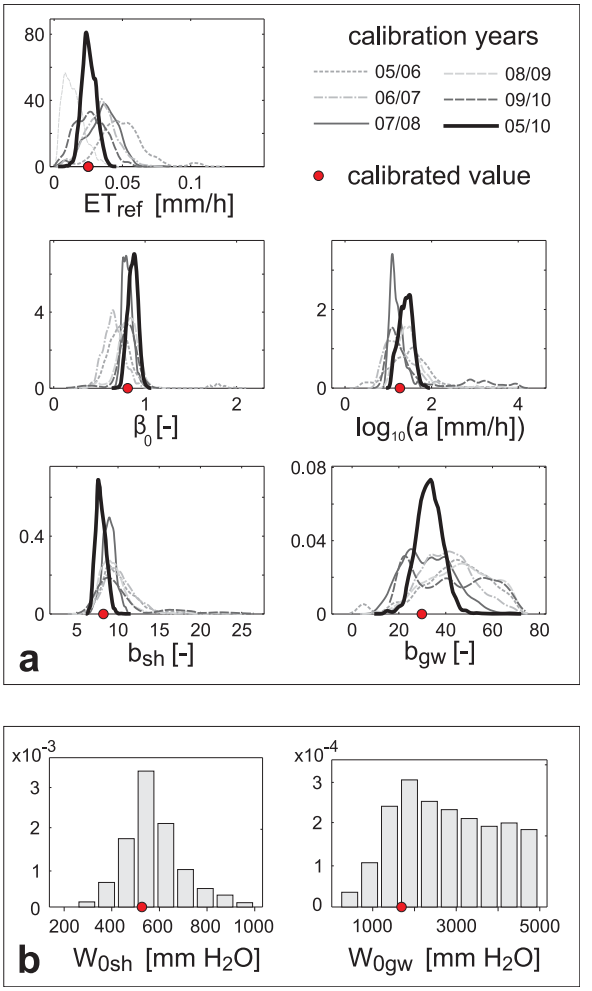

Figure 6. Posterior distributions of (a) hydrologic parameters and (b) residual storage volumes. Red dots indicate calibrated values (Table 2). The units on the *y* axes are relative number per *x* axis unit.

Similarly, the positive concentration peaks around January 2008 are properly caught in the simulation. This indicates that both the behaviors emerging from the observed time series (increased/decreased concentrations in response to floods) are reasonably represented by the model. NS efficiency of the best performance is 0.69.

The perceptual picture suggested by the model results is the following: during base flow conditions, discharge and solute concentrations are mostly sustained by groundwater flow, whereas right after storm events, water from the soil and highly fractured bedrock is mainly responsible for runoff formation, so the concentration at the outlet promptly shifts toward the concentration in the shallow storage (which may be either higher or lower than groundwater's, depending on the season). Our analysis thus reinforces the conceptual hypothesis of *Neal et al.* [2012]. During recessions, streamflow concentration gradually shifts back to the groundwater concentration. Hence, high-frequency dynamics originate at the transition between shallow and deep-water control on streamflow, induced by incoming storm events. Depending on whether shallow storage concentrations are higher or lower than those of groundwater, new storms may cause dilutions (e.g., August–November 2008 period) or positive concentration peaks (e.g., January–April 2008). This can be observed in Figure 8, where average storage concentrations in the two compartments can be identified as the end-members of the observed chloride fluctuations. Figure 8 also explains the reason that the groundwater storage volume is highly uncertain [*Seeger and Weiler*, 2014]: a bigger storage would result in nearly the same constant groundwater concentration, so the size of residual groundwater store is difficult to constrain by calibration. Nonetheless it is encouraging that the calibrated residual storage in the shallow and deep reservoirs implies a mean travel time of roughly 1.5 years, broadly consistent with the mean travel time of 0.9 years estimated independently for the Hafren catchment by *Kirchner et al.* [2000] using spectral analysis of longer-term (but less detailed) chloride time series.

Table 3. Nash-Sutcliffe Efficiencies (for Hourly Discharge) of the Calibrated Hydrologic Model

Year	E (1 Year Calib.)	E (5 Years Calib.)
2005/2006	0.89	0.88
2006/2007	0.92	0.91
2007/2008	0.94	0.94
2008/2009	0.87	0.85
2009/2010	0.82	0.82
2005/2010		0.90

Though very simple, our model is able to reproduce the main chloride dynamics reasonably well, suggesting that the resulting flow partitioning is a reasonable representation of the catchment behaviors. Our results indicate that streamflow concentration dynamics can be inferred from spatially integrated storage concentrations within

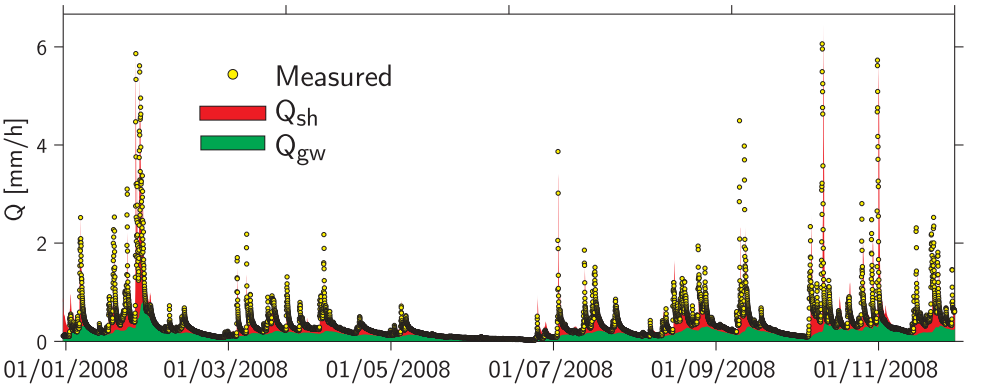

Figure 7. Measured and simulated discharge time series.

prescribed hydrologic compartments, even though these may not necessarily be mixed. From a physical viewpoint, this can be attributed to the pronounced heterogeneity of water velocities and flow paths that supply water to the stream network, resulting in enhanced mixing of waters originating from different source areas [*Kirchner et al.*, 2001].

Note that, as shown by *Neal et al.* [2012], the presence of both positive and negative peaks in the concentration is peculiar to chloride in this system because it is a conservative tracer whose input concentration fluctuates around a nearly constant long-term average. This implies that modeled shallow and deep storage concentrations cross each other during the year (see, e.g., Figure 8 before and after day 190). For other solutes, this might not be the case, because the concentration could be persistently lower in groundwater than in shallow storage (e.g., due to degradation processes, like for phosphorus), leading to positive concentration peaks in stormflow, or persistently higher in groundwater than in shallow storage (because of, e.g., rock weathering, like for silica), leading to negative peaks (i.e., dilution) in stormflow. Even for nonreactive tracers, one might observe persistent positive or negative concentration peaks if the input loads exhibit long-term nonstationarity. This was observed for chloride in the Hupsel Brook Catchment [*van der Velde et al.*, 2010], where soil water is systematically less concentrated than groundwater because of the reduction of fertilization loads during the last decades, induced by environmental policies.

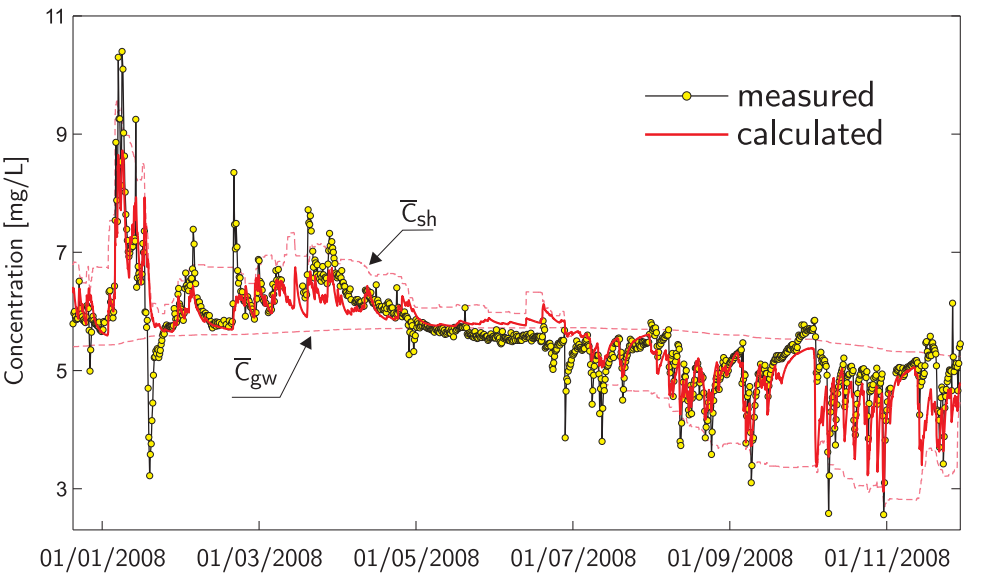

Figure 8. Measured and simulated chloride concentration time series. The dashed lines show the simulated mean concentrations of the shallow storage $\bar{C}_{sh}(t)$ and groundwater storage $\bar{C}_{gw}(t)$.

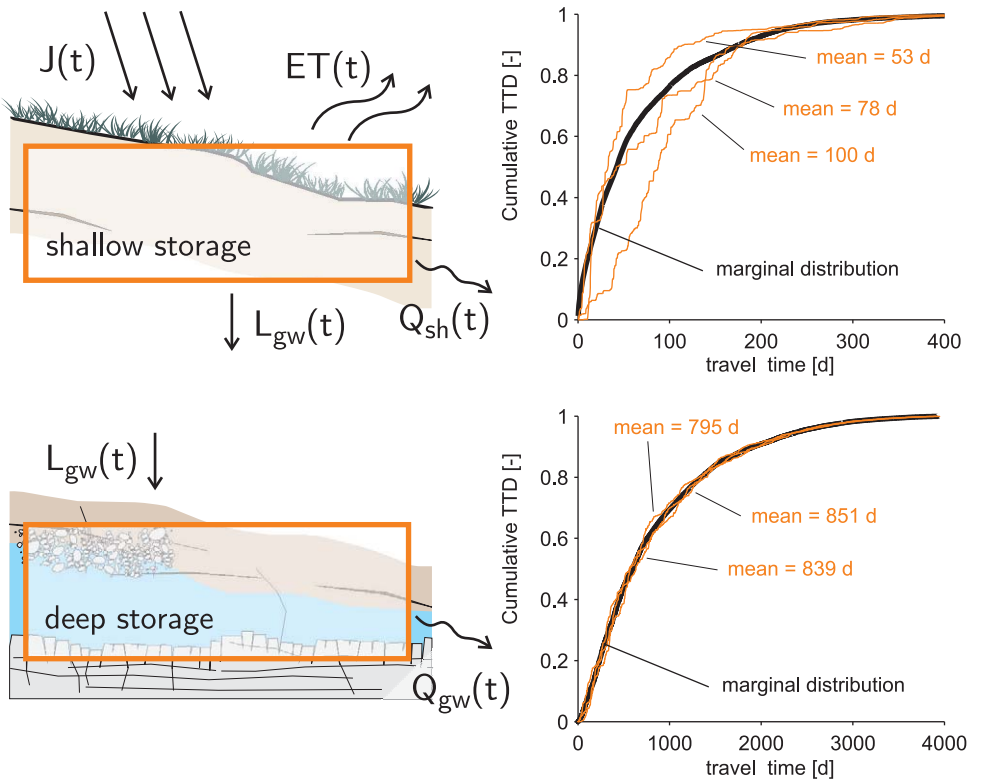

Figure 9. Example of three individual cumulative TTDs drawn from the shallow and deep storages, compared to the corresponding marginal distribution $p_m(T)$. The distributions are taken on 14 June 2008 (mean values 100 and 839 days), 16 September 2008 (mean values 78 and 851 days), and 20 November 2008 (mean values 53 and 795 days).

6. Travel Time Analysis

Backward travel time distributions over the simulation period 2007–2008 were reconstructed based on the equations described in section 3, using the total storage $W=S+W_0$ as the storage term in equation (2). Because backward distributions are based on precipitation events that happened up to many years before the considered period, the hydrochemical model was run from 1985 to 2008, to provide an estimate of all the hydrologic fluxes required for TTD computation. In order to balance between numerical efforts and accuracy in calculating TTDs, distributions were computed on 6 h time step.

For each individual storage (shallow and deep), the age distributions in the storage and in the outflows coincide, as prescribed by the adopted RS mixing scheme. In the shallow layer, TTDs (and hence RTDs) show enhanced time variance due to the high variability in flows and storages. Groundwater TTDs are, by contrast, relatively constant because flow variability is damped owing to the large storage size. This can be seen in Figure 9, where a few TTDs are reported for individual points in the time series and compared to the stationary marginal distributions. While individual distributions in the shallow layer show large departures from the corresponding marginal distribution, groundwater distributions are almost indistinguishable.

It is worth highlighting that when one considers the catchment as a whole, the overall system is far from being randomly sampled. This is because the shallow storage makes only a small contribution to total storage, but it is preferentially sampled by discharge, especially during high flows. The difference between the age distributions of the overall storage and discharge can be seen in Figure 10, where all cumulative distributions obtained during the simulation period are plotted. Two main features clearly emerge: (i) cumulative TTDs are generally shifted upward with respect to their corresponding RTDs, meaning that discharge is mostly made up of younger water than storage, and (ii) TTDs are much more variable over time, as shown by the larger range spanned by their mean values (inset). Discharge can release both very young waters (during storm events) and old waters (during dry periods), while total storage is always dominated by old waters contained in the deep storage.

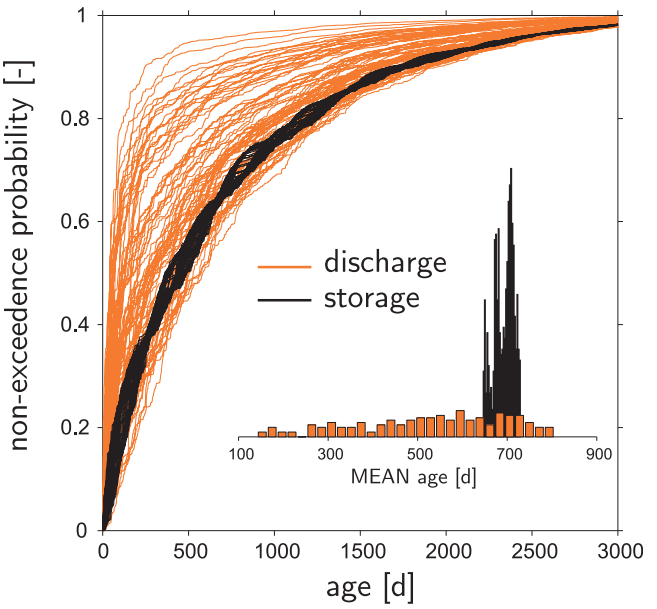

Figure 10. Cumulative age distributions in the overall water storage (shown in black) and discharge (shown in red). The distributions consider the combined effect of the shallow and deep systems. Each distribution corresponds to a different time of the simulation period. The inset reports the pdf of the mean values of the evolving distributions.

The difference between discharge and storage age dynamics is best explained by looking at the corresponding SAS functions ω (equation (1)). The functions were computed as the TTD/RTD ratio and then rescaled over the transformed residence time domain proposed by *van der Velde et al*. [2012] and shown in Appendix C. Such a change of variables conveys notable advantages because, in the transformed domain, the Stor-Age Selection functions turn into probability density functions and display a more regular and smooth shape. The SAS functions are reported in Figure 11, where different colors are used for different shapes. The same color is used to identify the corresponding shallow storage level (inset). The plot suggests that during wet conditions outflows have a preference for younger waters, and that this tendency is enhanced with increasing wetness. Conversely, when the catchment becomes dry, older water parcels tend to be preferentially sampled because the shallow system becomes almost inactive. The link between age-selection and storage, however, is not one-to-one because the system is characterized by some degree of hysteresis. The same storage can correspond to different catchment conditions, depending on whether the catchment is wetting or drying. This is visible in Figure 11 where similar age-selection functions (i.e., similar colors of curves) correspond to different shallow storage states (e.g., during peaks or recessions). Therefore, SAS functions can provide useful insights for the characterization of the hydrologic state of a watershed.

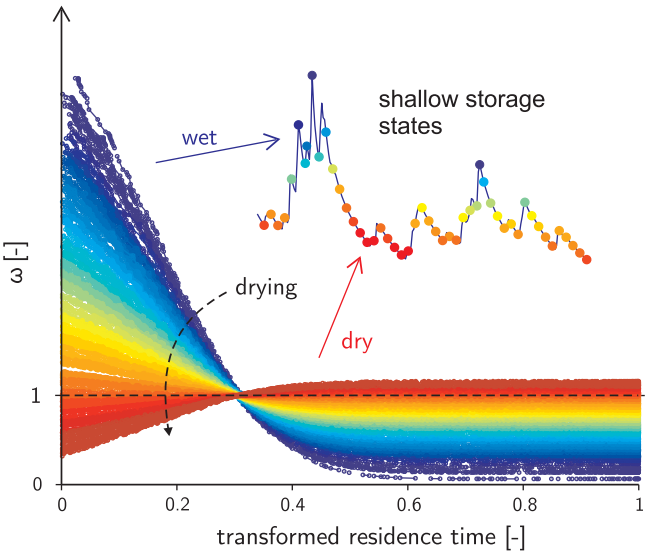

Figure 11. SAS functions computed over the whole simulation period. The color scheme links the functions with their corresponding (shallow) storage state.

So far, each TTD is representative of one simulation time step, regardless of the amount of discharge water it refers to, but one may want to get flow-weighted distributions that are more representative of the masses of water that leave the catchment. As higher discharges are characterized by younger water, flow-weighted average travel times are younger than time-weighted averages [*Peters et al*., 2013]. Marginal travel time distributions are intrinsically flow-weighted functions because individual TTDs are averaged out by weighting them by the corresponding discharge value. We calculated the

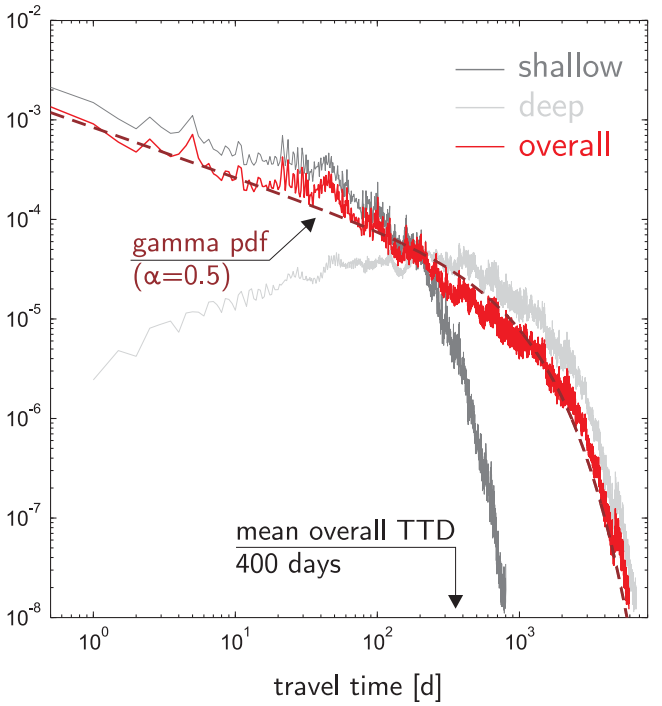

Figure 12. Marginal travel time distributions for the shallow subsurface flow, deep groundwater, and overall discharge. The overall marginal distribution is compared to a gamma pdf with shape parameter $\alpha=0.5$ and mean value 400 days (which is the same as the overall distribution).

marginal distributions using equation (A(1)) over the whole simulation period to explore the time-integrated behavior of the TTDs. Distributions computed for the shallow storage, groundwater, and overall discharge are compared in Figure 12. The plot shows that shallow-storage and groundwater distributions are characterized by different time scales (a few months and a few years, respectively), while the overall marginal distribution displays a smooth transition between shallow-storage and groundwater distributions, and hence spans a wide range of time scales. Interestingly, the overall marginal TTD closely resembles a Gamma pdf with shape parameter $\alpha=0.5$, which has often emerged from analyses of tracer time series using spectral methods to estimate stationary travel time distributions [*Kirchner et al.*, 2000, 2001; *Godsey et al.*, 2010; *Kirchner and Neal*, 2013].

Notwithstanding uncertainties involved in the spatial variability of chloride deposition, the travel time analysis allows for preliminary inferences about the catchment mass balance. The measurements suggest that during the study period a total of 15.7 g/m^2 entered the catchment through atmospheric deposition and 16.0 g/m^2 left the catchment as discharge (very close to the value of 16.5 g/m^2 predicted by the calibrated model). However, the close match between input and output mass only reflects the equilibrium between deposition and mass displaced from the catchment during the considered 11 months, without implying any balance closure in a kinematic sense. Indeed, the kinematic picture provided by the travel time analysis suggests that 55% of the total mass removed by discharge during the simulation period was already stored within the catchment before the start of that period.

A word of caution is needed at this point. The travel time analysis is based on the underlying hydrochemical model, so one may want to assess the impact of model parameters and the related uncertainty on estimated travel times. While a complete sensitivity analysis would be a time-consuming task left for future work, informal analyses showed general stability of travel time distributions under different parameter combinations. The only parameter which could have a substantial impact on travel times is the groundwater residual storage $W_{0_{gw}}$, because it does not have a clearly definable upper bound (see section 4.3). However, larger $W_{0_{gw}}$ values would leave the fundamental interaction between shallow and deep system (and hence the age-selection) unchanged, and its effect would be limited to increased groundwater ages, without affecting the overall patterns of behavior outlined by our results.

7. Conclusions

The major conclusions of this study are:

1. The hydrochemical model, based on a reasonable conceptualization of the Upper Hafren catchment, could accurately reproduce its hydrologic and chemical response. This allowed us to estimate the storages involved in solute mixing, and enabled us to infer dynamic travel time distributions.

2. Most of the high-frequency fluctuations in the measured chloride concentration of stream water can be explained by the sharp transition between groundwater flows (with an almost constant Cl concentration) and faster flows originating from shallower storage layers (with higher or lower concentration, as driven by the inter-seasonal variability of atmospheric inputs). The same transition in dominance between deep and shallow storage also drives large fluctuations in the mean age of stream water.
3. Emerging age-selection patterns indicate a clear preference of discharge for the youngest ages in storage. Such a preference is enhanced when the catchment is wet and faster flows dominate the hydrologic response, thereby implying that discharge is always younger than storage.

Our results support the coupled use of solute measurements and transport models to quantify catchment-scale mixing processes and interpret hydrochemical data sets. The dynamic TTD analysis, which is the essence of this approach, represents a fruitful way forward for catchment-scale transport studies.

Appendix A: Marginal TTD

The marginal TTD represents the probability of observing a particular travel time during the considered observation period, and can be computed as:

$$p_m(T) = \int_\Gamma p_Q(T/t) f(t)\, dt \tag{A1}$$

where Γ is the observation period for the averaging and $f(t)$ is a weighting function, in this case representing the probability of observing a particular exit time (t). In fact, $f(t)$ is proportional to $Q(t)$, because the higher the discharge at time t, the higher the probability of having many particles leaving the catchment at that time. Hence, the normalized discharge time series over Γ can be used in $f(t)$ and the marginal pdf basically serves as a flow-weighted average TTD.

Appendix B: Chloride Input Adjustments

In order to capture even small rainfall events, the autosampler was designed to have a large (57.5 cm) funnel which drained into a small (308 mL) bottle [*Neal et al.*, 2012], approximately corresponding to 1.2 mm of precipitation during the 7 h sampling interval. Hence, all rainfall events larger than 1.2 mm per 7 h produced some overflow. Because the initial part of the precipitation is usually higher in chloride due to the atmospheric (and funnel) washout, and given that the degree of mixing in such conditions is not well defined, samples taken during such events might not be representative of the average 7 h precipitation. During the modeled period (December 2007 to November 2008), 37% of the rainfall events exceeded 1.2 mm per 7 h (9% exceeded 10 mm), requiring the determination of the corresponding overflow concentration. A simple estimation method is to assign a virtual concentration that matches the mass balance with weekly chloride measurements taken at the same location with a different instrument [see *Neal et al.*, 2011]. This procedure is consistent with mass balance, but tends to flatten concentration values toward the corresponding weekly average. For this reason, we decided to adjust precipitation volumes only exceeding a suitable threshold value larger than 1.2 mm. After some preliminary tests using different thresholds, the final value was 5 mm that required the adjustment of 16% of the sampled concentrations.

Appendix C: The Transformed Residence Time Domain

The regular residence time might sometimes be inconvenient for representing SAS functions, as it induces large and irregular gaps corresponding to ages that are not present within the storage. For this reason, *van der Velde et al.* [2012] proposed the use of the cumulative residence time distribution $P_S(T,t)$ as a transformed residence time domain for the SAS functions:

$$T \mapsto P_S(T,t) = \int_0^T p_S(\tau,t) d\tau \tag{C1}$$

The new time domain is bounded in $[0, 1]$ as implied by the cumulative pdf. Therein, every point represents a fraction of storage sorted by age. SAS functions in the transformed domain are derived distributions, hence they become probability density functions:

$$\int_0^1 \omega(P_S, t)\, dP_S = 1 \tag{C2}$$

Acknowledgments
Data to support this article are from the Centre for Ecology and Hydrology (CEH) and are available through their Information Gateway or upon request. The authors wish to thank the Editors, Allan Rodhe, and two anonymous reviewers for their constructive comments. A.R. wishes to thank support from SNF-FNS Projects 200021-124930/1 and 200021-135241.

References

Ali, M., A. Fiori, and D. Russo (2014), A comparison of travel-time based catchment transport models, with application to numerical experiments, *J. Hydrol.*, *511*(2014), 605–618, doi:10.1016/j.jhydrol.2014.02.010.

Anderson, S., W. Dietrich, and G. Brimhall (2002), Weathering profiles, mass-balance analysis, and rates of solute loss: Linkages between weathering and erosion in a small, steep catchment, *Geol. Soc. Am. Bull.*, *114*(9), 1143–1158.

Benettin, P., A. Rinaldo, and G. Botter (2013a), Kinematics of age mixing in advection-dispersion models, *Water Resour. Res.*, *49*, 8539–8551, doi:10.1002/2013WR014708.

Benettin, P., Y. van der Velde, S. E. A. T. M. van der Zee, A. Rinaldo, and G. Botter (2013b), Chloride circulation in a lowland catchment and the formulation of transport by travel time distributions, *Water Resour. Res.*, *49*, 4619–4632, doi:10.1002/wrcr.20309.

Bertuzzo, E., M. Thomet, G. Botter and A. Rinaldo (2013), Catchment-scale herbicides transport: Theory and application, *Adv. Water Resour.*, *52*, 232–242, doi:10.1016/j.advwatres.2012.11.007.

Birkel, C., C. Soulsby, and D. Tetzlaff (2011), Modelling catchment-scale water storage dynamics: Reconciling dynamic storage with tracer-inferred passive storage, *Hydrol. Processes*, *25*(25), 3924–3936, doi:10.1002/hyp.8201.

Birkel, C., C. Soulsby, D. Tetzlaff, S. Dunn, and L. Spezia (2012), High-frequency storm event isotope sampling reveals time-variant transit time distributions and influence of diurnal cycles, *Hydrol. Processes*, *26*(2), 308–316, doi:10.1002/hyp.8210.

Birkel, C., C. Soulsby, and D. Tetzlaff (2015), Conceptual modelling to assess how the interplay of hydrological connectivity, catchment storage and tracer dynamics controls nonstationary water age estimates, *Hydrol. Processes*, doi:10.1002/hyp.10414, in press.

Botter, G. (2012), Catchment mixing processes and travel time distributions, *Water Resour. Res.*, *48*, W05545, doi:10.1029/2011WR011160.

Botter, G., T. Settin, M. Marani, and A. Rinaldo (2006), A stochastic model of nitrate transport and cycling at basin scale, *Water Resour. Res.*, *42*, W04415, doi:10.1029/2005WR004599.

Botter, G., A. Porporato, I. Rodriguez-Iturbe, and A. Rinaldo (2009), Nonlinear storage-discharge relations and catchment streamflow regimes, *Water Resour. Res.*, *45*, W10427, doi:10.1029/2008WR007658.

Botter, G., E. Bertuzzo, and A. Rinaldo (2010), Transport in the hydrologic response: Travel time distributions, soil moisture dynamics, and the old water paradox, *Water Resour. Res.*, *46*, W03514, doi:10.1029/2009WR008371.

Botter, G., E. Bertuzzo, and A. Rinaldo (2011), Catchment residence and travel time distributions: The master equation, *Geophys. Res. Lett.*, *38*, L11403, doi:10.1029/2011GL047666.

Brandt, C., M. Robinson, and J. W. Finch (2004), Anatomy of a catchment: The relation of physical attributes of the Plynlimon catchments to variations in hydrology and water status, *Hydrol. Earth Syst. Sci.*, *8*(3), 345–354, doi:10.5194/hess-8-345-2004.

Brooks, J. R., H. R. Barnard, R. Coulombe, and J. J. McDonnell (2010), Ecohydrologic separation of water between trees and streams in a Mediterranean climate, *Nat. Geosci.*, *3*(2), 100–104, doi:10.1038/ngeo722.

Brutsaert, W., and J. L. Nieber (1977), Regionalized drought flow hydrographs from a mature glaciated plateau, *Water Resour. Res.*, *13*(3), 637–643, doi:10.1029/WR013i003p00637.

Cvetkovic, V., C. Carstens, J.-O. Selroos, and G. Destouni (2012), Water and solute transport along hydrological pathways, *Water Resour. Res.*, *48*, W06537, doi:10.1029/2011WR011367.

Danckwerts, P. (1953), Continuous flow systems: Distribution of residence times, *Chem. Eng. Sci.*, *2*(1), 1–13.

Davies, J., K. Beven, A. Rodhe, L. Nyberg, and K. Bishop (2013), Integrated modeling of flow and residence times at the catchment scale with multiple interacting pathways, *Water Resour. Res.*, *49*, 4738–4750, doi:10.1002/wrcr.20377.

Detty, J. M., and K. J. McGuire (2010), Threshold changes in storm runoff generation at a till-mantled headwater catchment, *Water Resour. Res.*, *46*, W07525, doi:10.1029/2009WR008102.

Gannon, J. P., S. W. Bailey, and K. J. McGuire (2014), Organizing groundwater regimes and response thresholds by soils: A framework for understanding runoff generation in a headwater catchment, *Water Resour. Res.*, *50*, 8403–8419, doi:10.1002/2014WR015498.

Godsey, S. E., J. W. Kirchner and D. W. Clow (2009), Concentration-discharge relationships reflect chemostatic characteristics of US catchments, *Hydrol. Processes*, *23*(13), 1844–1864, doi:10.1002/hyp.7315.

Godsey, S. E., et al. (2010), Generality of fractal 1/f scaling in catchment tracer time series, and its implications for catchment travel time distributions, *Hydrol. Processes*, *24*(12), 1660–1671, doi:10.1002/hyp.7677.

Haria, A., and P. Shand (2004), Evidence for deep sub-surface flow routing in forested upland Wales: Implications for contaminant transport and stream flow generation, *Hydrol. Earth Syst. Sci.*, *8*(3), 334–344.

Haria, A. H., and P. Shand (2006), Near-stream soil waterroundwater coupling in the headwaters of the Afon Hafren, Wales: Implications for surface water quality, *J. Hydrol.*, *331*(3-4), 567–579, doi:10.1016/j.jhydrol.2006.06.004.

Harman, C. and M. Kim (2014), An efficient tracer test for time-variable transit time distributions in periodic hydrodynamic systems, *Geophys. Res. Lett.*, *41*, 1567–1575, doi:10.1002/2013GL058980.

Harman, C. J. (2015), Time-variable transit time distributions and transport: Theory and application to storage-dependent transport of chloride in a watershed, *Water Resour. Res.*, *51*, 1–30, doi:10.1002/2014WR015707.

Heidbuechel, I., P. A. Troch, S. W. Lyon, and M. Weiler (2012), The master transit time distribution of variable flow systems, *Water Resour. Res.*, *48*, W06520, doi:10.1029/2011WR011293.

Hrachowitz, M., H. Savenije, T. A. Bogaard, D. Tetzlaff, and C. Soulsby (2013), What can flux tracking teach us about water age distribution patterns and their temporal dynamics?, *Hydrol. Earth Syst. Sci.*, *17*(2), 533–564, doi:10.5194/hess-17-533-2013.

Kirby, C., M. Newson, and K. Gilman (1991), *Plynlimon Research: The First Two Decades*, vol. 109, Inst. of Hydrol., Wallingford, U. K.

Kirby, C., C. Neal, H. Turner, and P. Moorhouse (1997), A bibliography of hydrological, geomorphological, sedimentological, biological and hydrochemical references to the Institute of Hydrology experimental catchment studies in Plynlimon, *Hydrol. Earth Syst. Sci.*, *1*(3), 755–763.

Kirchner, J., X. Feng and C. Neal (2000), Fractal stream chemistry and its implications for contaminant transport in catchments, *Nature*, *403*(6769), 524–527, doi:10.1038/35000537.
Kirchner, J., X. Feng, and C. Neal (2001), Catchment-scale advection and dispersion as a mechanism for fractal scaling in stream tracer concentrations, *J. Hydrol.*, *254*(1-4), 82–101, doi:10.1016/S0022-1694(01)00487-5.
Kirchner, J. W. (2009), Catchments as simple dynamical systems: Catchment characterization, rainfall-runoff modeling, and doing hydrology backward, *Water Resour. Res.*, *45*, W02429, doi:10.1029/2008WR006912.
Kirchner, J. W. and C. Neal (2013), Universal fractal scaling in stream chemistry and its implications for solute transport and water quality trend detection, *Proc. Natl. Acad. Sci. U. S. A.*, *110*(30), 12,213–12,218, doi:10.1073/pnas.1304328110.
Kirchner, J. W., D. Tetzlaff, and C. Soulsby (2010), Comparing chloride and water isotopes as hydrological tracers in two Scottish catchments, *Hydrol. Processes*, *24*(12), 1631–1645, doi:10.1002/hyp.7676.
Kreft, A., and A. Zuber (1978), On the physical meaning of the dispersion equation and its solutions for different initial and boundary conditions, *Chem. Eng. Sci.*, *33*(11), 1471–1480, doi:10.1016/0009-2509(78)85196-3.
Marc, V., and M. Robinson (2007), The long-term water balance (19722004) of upland forestry and grassland at Plynlimon, mid-Wales, *Hydrol. Earth Syst. Sci.*, *11*(1), 44–60, doi:10.5194/hess-11-44-2007.
McGuire, K. J., and J. J. McDonnell (2006), A review and evaluation of catchment transit time modeling, *J. Hydrol.*, *330*(3-4), 543–563, doi:10.1016/j.jhydrol.2006.04.020.
McMillan, H., D. Tetzlaff, M. Clark, and C. Soulsby (2012), Do time-variable tracers aid the evaluation of hydrological model structure? A multimodel approach, *Water Resour. Res.*, *48*, W05501, doi:10.1029/2011WR011688.
Neal, C. (2004), The water quality functioning of the upper River Severn, Plynlimon, mid-Wales: Issues of monitoring, process understanding and forestry, *Hydrol. Earth Syst. Sci.*, *8*(3), 521–532.
Neal, C., and J. Kirchner (2000), Sodium and chloride levels in rainfall, mist, streamwater and groundwater at the Plynlimon catchments, mid-Wales: Inferences on hydrological and chemical controls, *Hydrol. Earth Syst. Sci.*, *4*(2), 295–310.
Neal, C., et al. (1997), The occurrence of groundwater in the Lower Palaeozoic rocks of upland Central Wales, *Hydrol. Earth Syst. Sci.*, *1*, 3–18.
Neal, C., B. Reynolds, M. Neal, B. Pugh, L. Hill, and H. Wickham (2001), Long-term changes in the water quality of rainfall, cloud water and stream water for moorland, forested and clear-felled catchments at Plynlimon, mid-Wales, *Hydrol. Earth Syst. Sci.*, *5*(3), 459–476, doi:10.5194/hess-5-459-2001.
Neal, C., M. Robinson, B. Reynolds, M. Neal, P. Rowland, S. Grant, D. Norris, B. Williams, D. Sleep, and A. Lawlor (2010), Hydrology and water quality of the headwaters of the River Severn: Stream acidity recovery and interactions with plantation forestry under an improving pollution climate, *Sci. Total Environ.*, *408*(21), 5035–5051, doi:10.1016/j.scitotenv.2010.07.047.
Neal, C., et al. (2011), Three decades of water quality measurements from the Upper Severn experimental catchments at Plynlimon, Wales: An openly accessible data resource for research, modelling, environmental management and education, *Hydrol. Processes*, *25*(24), 3818–3830, doi:10.1002/hyp.8191.
Neal, C., et al. (2012), High-frequency water quality time series in precipitation and streamflow: From fragmentary signals to scientific challenge, *Sci. Total Environ.*, *434*(SI), 3–12, doi:10.1016/j.scitotenv.2011.10.072.
Neal, C., et al. (2013), High-frequency precipitation and stream water quality time series from Plynlimon, Wales: An openly accessible data resource spanning the periodic table, *Hydrol. Processes*, *27*(17), 2531–2539, doi:10.1002/hyp.9814.
Niemi, A. J. (1977), Residence time distributions of variable flow processes, *Int. J. Appl. Radiat. Isotopes*, *28*(10-11), 855–860, doi:10.1016/0020-708X(77)90026-6.
Oda, T., Y. Asano, and M. Suzuki (2009), Transit time evaluation using a chloride concentration input step shift after forest cutting in a Japanese headwater catchment, *Hydrol. Processes*, *23*, 2705–2713, doi:10.1002/hyp.7361.
Page, T., K. Beven, J. Freer, and C. Neal (2007), Modelling the chloride signal at Plynlimon, Wales, using a modified dynamic TOPMODEL incorporating conservative chemical mixing (with uncertainty), *Hydrol. Processes*, *21*(3), 292–307, doi:10.1002/hyp.6186.
Park, J., H. E. Gall, D. Niyogi, and P. S. C. Rao (2013), Temporal trajectories of wet deposition across hydro-climatic regimes: Role of urbanization and regulations at U.S. and east Asia sites, *Atmos. Environ.*, *70*, 280–288, doi:10.1016/j.atmosenv.2013.01.033.
Penna, D., O. Oliviero, R. Assendelft, G. Zuecco, I. H. J. V. Meerveld, T. Anfodillo, V. Carraro, M. Borga, and G. D. Fontana (2013), Tracing the water sources of trees and streams: Isotopic analysis in a small pre-alpine catchment, *Procedia Environ. Sci.*, *19*, 106–112, doi:10.1016/j.proenv.2013.06.012.
Peters, N. E., D. A. Burns, and B. T. Aulenbach (2013), Evaluation of high-frequency mean streamwater transit-time estimates using groundwater age and dissolved silica concentrations in a small forested watershed, *Aquat. Geochem.*, *20*(2-3), 183–202, doi:10.1007/s10498-013-9207-6.
Queloz, P., E. Bertuzzo, L. Carraro, G. Botter, F. Miglietta, P. Rao, and A. Rinaldo (2015a), Transport of fluorobenzoate tracers in a vegetated hydrologic control volume: 1. Experimental results, *Water Resour. Res.*, doi:10.1002/2014WR016433, in press.
Queloz, P., L. Carraro, P. Benettin, G. Botter, A. Rinaldo, and E. Bertuzzo (2015b), Transport of fluorobenzoate tracers in a vegetated hydrologic control volume: 2. Theoretical inferences and modeling, *Water Resour. Res.*, doi:10.1002/2014WR016508, in press.
Rinaldo, A., and A. Marani (1987), Basin scale-model of solute transport, *Water Resour. Res.*, *23*(11), 2107–2118, doi:10.1029/WR023i011p02107.
Rinaldo, A., A. Marani, and R. Rigon (1991), Geomorphological Dispersion, *Water Resour. Res.*, *27*(4), 513–525.
Rinaldo, A., K. J. Beven, E. Bertuzzo, L. Nicotina, J. Davies, A. Fiori, D. Russo, and G. Botter (2011), Catchment travel time distributions and water flow in soils, *Water Resour. Res.*, *47*, W07537, doi:10.1029/2011WR010478.
Seeger, S., and M. Weiler (2014), Lumped convolution integral models revisited: On the meaningfulness of inter catchment comparisons, *Hydrol. Earth Syst. Sci. Discuss.*, *11*(6), 6753–6803, doi:10.5194/hessd-11-6753-2014.
Shand, P., A. H. Haria, C. Neal, K. J. Griffiths, D. C. Gooddy, A. J. Dixon, T. Hill, D. K. Buckley, and J. E. Cunningham (2005), Hydrochemical heterogeneity in an upland catchment: Further characterisation of the spatial, temporal and depth variations in soils, streams and groundwaters of the Plynlimon forested catchment, Wales, *Hydrol. Earth Syst. Sci.*, *9*(6), 621–644, doi:10.5194/hess-9-621-2005.
Shaw, S. B., A. A. Harpold, J. C. Taylor, and M. T. Walter (2008), Investigating a high resolution, stream chloride time series from the Biscuit Brook catchment, Catskills, NY, *J. Hydrol.*, *348*(3-4), 245–256, doi:10.1016/j.jhydrol.2007.10.009.
Smith, T., L. Marshall, B. McGlynn, and K. Jencso (2013), Using field data to inform and evaluate a new model of catchment hydrologic connectivity, *Water Resour. Res.*, *49*, 6834–6846, doi:10.1002/wrcr.20546.
Svensson, T., G. M. Lovett, and G. E. Likens (2012), Is chloride a conservative ion in forest ecosystems?, *Biogeochemistry*, *107*(1-3), 125–134, doi:10.1007/s10533-010-9538-y.
ter Braak, C. J. F., and J. A. Vrugt (2008), Differential evolution Markov Chain with snooker updater and fewer chains, *Stat. Comput.*, *18*(4), 435–446, doi:10.1007/s11222-008-9104-9.

Tetzlaff, D., C. Birkel, J. Dick, J. Geris, and C. Soulsby (2014), Storage dynamics in hydropedological units control hillslope connectivity, runoff generation, and the evolution of catchment transit time distributions, *Water Resour. Res.*, *50*, 969–985, doi:10.1002/2013WR014147.

Thompson, S. E., N. B. Basu, J. Lascurain, A. Aubeneau, and P. S. C. Rao (2011), Relative dominance of hydrologic versus biogeochemical factors on solute export across impact gradients, *Water Resour. Res.*, *47*, W00J05, doi:10.1029/2010WR009605.

van der Velde, Y., G. H. de Rooij, J. C. Rozemeijer, F. C. van Geer, and H. P. Broers (2010), Nitrate response of a lowland catchment: On the relation between stream concentration and travel time distribution dynamics, *Water Resour. Res.*, *46*, W11534, doi:10.1029/2010WR009105.

van der Velde, Y., P. J. J. F. Torfs, S. E. A. T. M. van der Zee, and R. Uijlenhoet (2012), Quantifying catchment-scale mixing and its effect on time-varying travel time distributions, *Water Resour. Res.*, *48*, W06536, doi:10.1029/2011WR011310.

van der Velde, Y., I. Heidbuchel, S. W. Lyon, L. Nyberg, A. Rodhe, K. Bishop, and P. A. Troch (2015), Consequences of mixing assumptions for time-variable travel time distributions, *Hydrol. Processes*, doi:10.1002/hyp.10372, in press.

Vrugt, J., C. T. Braak, C. Diks, B. Robinson, J. Hyman, and D. Higdon (2009), Accelerating Markov chain Monte Carlo simulation by differential evolution with self-adaptive randomized subspace sampling, *Int. J. Nonlinear Sci. Numer. Simul.*, *10*(3), 271–288.

Xu, G., H. Magen, J. Tarchitzky, and U. Kafkafi (1999), Advances in chloride nutrition of plants, *Adv. Agron.*, *68*, 97–150, doi:10.1016/S0065-2113(08)60844-5.

Erratum

In the previously published version of the paper, two citations to "*Harman*, 2014" should instead be in reference to "*Harman*, 2015." These citations have been corrected, and this may be considered the authoritative version of record.